ЖУРНАЛ СТРУКТУРНОЙ ХИМИИ

2017. Том 58, № 7 *Сентябрь – октябрь* *С. 1316 – 1326*

UDC 541.6

THEORETICAL PREDICTIONS ON THE STRUCTURE AND *d*-AO-BASED AROMATICITY OF $Re_3F_3^{2+/0/4-}$, $Re_3F_3X^+$ (X = Li, Na, K), AND $Re_3F_3Y^{2+}$ (Y = Be, Mg, Ca) CLUSTERS

B. Jin[1], Q. Jin[2], F.K. Jin[3]

[1]*School of Environment and Biology Engineering, Shenyang University of Chemical Technology, Shenyang, P.R. China*
E-mail: jinbiao@syuct.edu.cn
[2]*School of Chemical Engineering, Beijing Institute of Petrochemical Technology, Beijing, P.R. China*
[3]*Liaoning University of Petroleum and Chemical Technology, Fushun, P.R. China*

Received November, 13, 2015 *Revised — July, 11, 2016*

The electronic structure and chemical bonding in $Re_3F_3^{2+/0/4-}$ clusters are investigated using density functional theory (DFT) calculations. Out research results show that the ground state for the $Re_3F_3^{2+/0/4-}$ clusters is found to be triplet state $^3A_1'$ with the D_{3h} symmetry, quintet state $^5A'$ with the C_s symmetry, and quintet state $^5A_1'$ with the D_{3h} symmetry, respectively. A detailed molecular orbital (MO) analysis reveals that the $Re_3F_3^{2+}$ (D_{3h}, $^3A_1'$) dication possesses multiple (π_F and partial δ_{Re}) aromaticity that is respectively responsible for the triangular F_3 framework and the triangular Re_3 framework in the $Re_3F_3^{2+}$ (D_{3h}, $^3A_1'$) dication. The neutral Re_3F_3 (C_s, $^5A'$) cluster possesses partial δ-aromaticity that is responsible for the triangular Re_3 framework in the Re_3F_3 (C_s, $^5A'$) cluster. The $Re_3F_3^{4-}$ (D_{3h}, $^5A_1'$) anion possesses multiple (σ and partial δ) aromaticity that is responsible for the triangular Re_3 framework in the $Re_3F_3^{4-}$ (D_{3h}, $^5A_1'$) cluster. We also examined their hexagonal pyramidal-type $Re_3F_3X^+$ (C_{3v}, $^1A_1'$) (X = Li, Na, K) and $Re_3F_3Y^{2+}$ (C_{3v}, $^1A_1'$) (Y = Be, Mg, Ca) complexes containing the Re_3F_3 (D_{3h}, $^1A_1'$) ligand to reveal that the Re_3F_3 (D_{3h}, $^1A_1'$) structural unit is perfectly preserved in these $Re_3F_3X^+$ (C_{3v}, $^1A_1'$) and $Re_3F_3Y^{2+}$ (C_{3v}, $^1A_1'$) complexes also having the corresponding *d*-orbital aromatic characters.

DOI: 10.26902/JSC20170703

K e y w o r d s: rhenium low-fluoride cluster, aromaticity, DFT calculations.

INTRODUCTION

A δ bond localized between the two Re atoms was first discovered in $K_2[Re^2Cl_8]\cdot 2H_2O$. Cotton and co-workers [1] reported this milestone research result which represented a new mode of chemical bonding in 1964. This work has also generated renewed interest in rhenium crystalline compounds. Before long, they reported one after another that the crystal structure of ReX_3 (X = Cl, Br, I) was composed of $Re(\mu\text{-}X)_3X_6$ subunits [2—4]. Rinke *et al.* [5—7] discovered that the ReX_3 (X = Cl, Br, I) compounds vaporized as $Re(\mu\text{-}X)_3X_6$ clusters in mass spectrometric experiments. In 2010, Sergeeva

and Boldyrev [8] performed the AdNDP analysis for $Re_3(\mu\text{-}X)_3X_6$ and $Re_3(\mu\text{-}X)_3X_6^{2-}$ (X = F, Cl, Br, I) clusters. Results of this analysis revealed that all neutral $Re_3(\mu\text{-}X)_3X_6$ (X = F, Cl, Br, I) species having Re = Re double bonds were not aromatic. For the $Re_3(\mu\text{-}X)_3X_6^{2-}$ (X = F, Cl, Br, I) dianions the AdNDP analysis revealed that the top sixteen full occupied valence orbitals in the $Re_3(\mu\text{-}X)_3X_6^{2-}$ (X = F, Cl, Br, I) dianions contained six 2*c*—2*e* Re—X σ bonds, three 3*c*—2*e* Re—X—Re σ bonds, three 2*c*—2*e* *d*-AO-based Re—Re σ bonds, three lone pairs (one on each Re atom), and one delocalized 3*c*—2*e* (HOMO) *d*-AO-based metal-metal π bond ([8] Fig. 9, *a*), which makes the dianion π aromaticity according to the (4*n*+2) Hückel rule for π aromaticity, while NICS(0) and NICS(1) suggest aromaticity in both $Re_3(\mu\text{-}X)_3X_6$ and $Re_3(\mu\text{-}X)_3X_6^{2-}$ (X = F, Cl, Br, I) clusters [9]. There are similar results of the research of Re_3X_9, $Re_3X_9^{2+}$ (X = Cl, Br) [8, 10, 11] and $[(XtRe)_3(\mu_2\text{—}X_6)]^+$ (X = Cl, Br, I) [12].

Rhenium oxides are of importance for their wide industrial applications, especially as industrial catalysts for olefin metatheses [13—15]. Structures, stabilities, and electronic properties of rhenium oxides together with bare rhenium clusters have been systematically investigated by experimental and theoretical methods. The number of rhenium oxides with aromatic/antiaromatic systems reported in the literature has grown enormously. Specially, mono-rhenium oxide clusters have been studied in a number of previous works, for example experimentally [16—20] and theoretically [17, 20, 21]: $Re(O_2)^+$, $Re(O_2)_2^+$, $Re(O_2)_3^+$, $Re(O_2)_4^+$, ReO_3^+, $ReO_3(O_2)^+$, ReO_5^+, and so on. Chen *et al.* [22] combined anion photoelectron spectroscopy (PES) with density functional theory (DFT) calculations to study the structures, bonding, and electronic properties in mono-rhenium oxide clusters: ReO_n and ReO_n^{2-} (*n* = 3—4). Zhai *et al*. [23] reported a PES and DFT study on the electronic structure and conflicting *d*-orbital aromaticity in trirhenium oxide cluster $Re_3O_3^-$. In addition, the structure, stabilities, and electronic properties of bare rhenium Re_n ($n \le 8$) clusters have been systematically investigated by DFT at the PBEPBE level employing SDD basis sets [24]. Obviously, rhenium compounds contain mainly rich-oxidation-state and low-oxidation-state transition metal compounds. We consider that δ aromaticity may exist in other multi-nuclear rhenium compounds. The $Re_3F_3^{2+/0/4-}$ clusters are derived from a transition metal low-fluoride conjecture cluster, and this drives the objective to be achieved at the DFT level.

We assume the counting rules for *d*-AO-based σ and π aromaticity to be 4*n*+4 (aromaticity) and (4*n*+6) (antiaromaticity) for a cyclic structure with an even number of transition metal atoms and (4*n*+2) (aromaticity) and 4*n* (antiaromaticity) for a cyclic structure with an odd number of transition metal atoms. The counting rule for *d*-AO-based δ aromaticity is (4*n*+2)/4*n* for aromaticity/antiaromaticity, respectively [25]. We call it the expanding (4*n*+2) Hückel counting rules for multiple aromaticity in transition metal clusters.

COMPUTATIONAL METHODS

All calculations were performed using the Gaussian 03 program package [26]. Equilibrium geometries and vibrational frequencies of the rhenium low-fluoride $Re_3F_3^{2+/0/4-}$ clusters and their hexagonal pyramidal-type $Re_3F_3X^+$ (C_{3v}, $^1A_1'$) (X = Li, Na, K) and $Re_3F_3Y^{2+}$ (C_{3v}, $^1A_1'$) (Y = Be, Mg, Ca) compounds were fully optimized using DFT-B3LYP [27—29] levels of theory with the 6-311++G** basis set for F, Li, Na, K, Be, Mg, Ca and the LANL2DZ basis set for heavier Re metals (*Z* = 75). Vibrational frequencies were calculated to characterize stationary points as the minima (number of imaginary frequencies $N_{imag} = 0$) or the transition states ($N_{imag} = 1$) and the second-order saddle points ($N_{imag} = 2$) by the B3LYP methods with the corresponding basis set. Molecular orbitals (MOs) for the most stable $Re_3F_3^{2+/0/4-}$ clusters, $Re_3F_3X^+$ (C_{3v}, $^1A_1'$) (X = Li, Na, K) and $Re_3F_3Y^{2+}$ (C_{3v}, $^1A_1'$) (Y = Be, Mg, Ca) complexes were calculated by the B3LYP method with the corresponding basis set. All MO pictures were made using the GaussView 3.0 program [26]. The bonding nature and

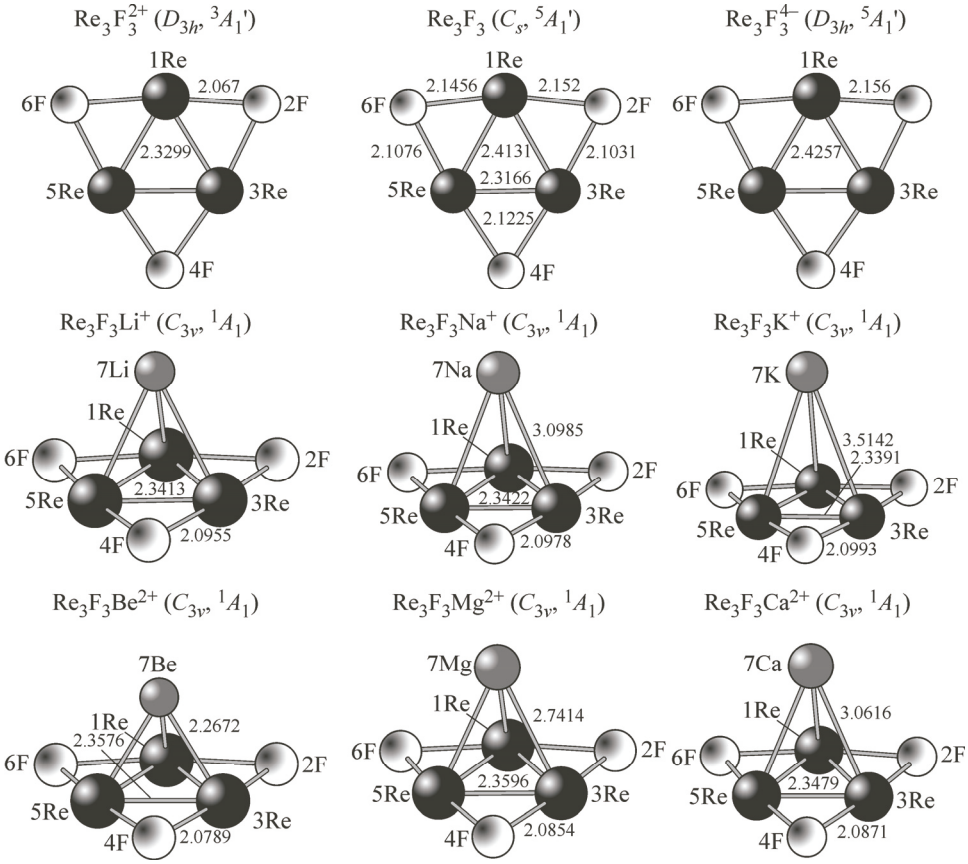

Fig. 1. Optimized structures for the ground states of the $Re_3F_3^{2+/0/4-}$ clusters and the minima of the $Re_3F_3X^+$ (C_{3v}, $^1A_1$) (X = Li, Na, K) and $Re_3F_3Y^{2+}$ (C_{3v}, $^1A_1$) (Y = Be, Mg, Ca) complexes at the B3LYP level of theory

atomic charge were analyzed by the natural bond orbital (NBO) [30, 31] using the B3LYP method with the corresponding basis set.

RESULTS AND DISCUSSION

The optimized geometric structures for the ground states of $Re_3F_3^{2+/0/4-}$ clusters and the minima of $Re_3F_3X^+$ (C_{3v}, $^1A_1'$) (X = Li, Na, K) and $Re_3F_3Y^{2+}$ (C_{3v}, $^1A_1'$) (Y = Be, Mg, Ca) complexes are illustrated in Fig. 1. Table 1 lists the lowest vibrational frequencies (γ_{min}), Wiberg bond indices of Re—Re ($WBI_{Re—Re}$) and Re—F ($WBI_{Re—F}$) bonds, total WBI of metal centers M (WBI_M), natural atomic charges of metal centers M (Q_M), and the relative energies ΔE or total energies E_T (kcal/mol) at the B3LYP level of theory for $Re_3F_3^{2+/0/4-}$ of selected low-lying isomers, $Re_3F_3X^+$(C_{3v}, $^1A_1$) (X = Li, Na, K) and $Re_3F_3Y^{2+}$ (C_{3v}, $^1A_1$) (Y = Be, Mg, Ca) clusters. The MOs pictures for the most stable $Re_3F_3^{2+}$ (D_{3h}, $^3A_1'$), Re_3F_3 (C_s, $^5A'$), and $Re_3F_3^{4-}$ (D_{3h}, $^5A_1'$) clusters are illustrated in Fig. 2. The MOs pictures for the most stable $Re_3F_3Li^+$ (C_{3v}, $^1A_1'$) and $Re_3F_3Be^{2+}$ (C_{3v}, $^1A_1'$) complexes are illustrated in Fig. 3 and the top nine MOs for the Re_3F_3 (D_{3h}, $^1A_1'$) cluster are given for comparison.

$Re_3F_3^{2+/0/4-}$ clusters. Geometric structures. We initially performed an extensive search for the $Re_3F_3^{2+/0/4-}$ global minimum for the singlet, triplet, quintet, and heptet states at the B3LYP level of theories. For the neutral, dication, and quadrivalent anion clusters we considered all different geometries and spin multiplicities. A selected set of optimized low-lying structures and electronic states for

Table 1

Calculated lowest vibrational frequencies (γ_{min}), *Wiberg bond index of the* Re—Re ($WBI_{Re—Re}$) *and* Re—F ($WBI_{Re—F}$) *bonds*, *total* WBIs *of metal centers* M (WBI_M), *natural atomic charges of metal centers* M (Q_M), *and relative energies* ΔE *or total energies* E_T (kcal/mol) *at the* B3LYP *level of theory for* $Re_3F_3^{2+/0/4-}$ *of selected low-lying isomers*, *the* $Re_3F_3X^+$ (C_{3v}, $^1A_1$) (X = Li, Na, K) *and* $Re_3F_3Y^{2+}$ (C_{3v}, $^1A_1$) (Y = Be, Mg, Ca) *clusters*

Species	γ_{min}, cm^{-1}	$l_{Re—Re}$, Å	$l_{Re—F}$, Å	$l_{Re—M}$, Å	$WBI_{Re—Re}$	$WBI_{Re—F}$	$\Delta E/E_T$, kcal/mol	WBI_M	Q_M,)
$Re_3F_3^{2+}$ (D_{3h}, $^3A_1'$)	99	2.330	2.067		1.940	0.370	0.000		
Re_3F_3 (D_{3h}, $^1A_1'$)	118	2.333	2.104		1.890	0.323	189.508		
Re_3F_3 (C_{2v}, $^3B_1$)	156	2.332~2.333	2.102~2.108		1.511~1.836	0.314~0.322	187.625		
Re_3F_3 (C_s, $^5A'$)	120	2.317~2.414	2.103~2.146		1.214~2.068	0.282~0.328	0.000		
Re_3F_3 (C_{2v}, $^7B_2$)	84	2.415~2.511	2.073~2.167		1.065~1.281	0.280~0.336	116.089		
$Re_3F_3^{4-}$ (D_{3h}, $^1A_1'$)	85	2.172	2.406		1.844	0.298	461.219		
$Re_3F_3^{4-}$ (D_{3h}, $^3A_1'$)	72	2.163	2.378		1.929	0.331	495.105		
$Re_3F_3^{4-}$ (C_{2v}, $^3B_2$)	67	2.167~2.186	2.322~2.167		1.624	0.307	85.341		
$Re_3F_3^{4-}$ (D_{3h}, $^5A_1'$)	128	2.156	2.426		1.464	0.293	0.000		
$Re_3F_3^{4-}$ (C_s, $^7A'$)	96	2.123~2.251	2.467~2.625		1.269	0.286	136.797		
$Re_3F_3Li^+$ (C_{3v}, $^1A_1$)	131	2.341	2.096	2.696	1.870	0.342	–341452.276	0.188	0.904
$Re_3F_3Na^+$ (C_{3v}, $^1A_1$)	74	2.342	2.098	3.099	1.875	0.338	–438576.931	0.122	0.938
$Re_3F_3K^+$ (C_{3v}, $^1A_1$)	55	2.339	2.099	3.514	1.879	0.335	–713209.862	0.064	0.968
$Re_3F_3Be^{2+}$ (C_{3v}, $^1A_1$)	131	2.358	2.079	2.267	1.804	0.373	–345681.634	1.090	1.348
$Re_3F_3Mg^{2+}$ (C_{3v}, $^1A_1$)	41	2.360	2.085	2.741	1.844	0.365	–462021.024	0.692	1.589
$Re_3F_3Ca^{2+}$ (C_{3v}, $^1A_1$)	62	2.348	2.087	3.062	1.854	0.358	–761708.365	0.477	1.754

the $Re_3F_3^{2+/0/4-}$ global minimum are summarized in Table 1. Table 1 presents their equilibrium geometries, relative energies, the lowest vibrational frequencies and interatomic distances at the B3LYP level of theory. Four geometric isomers of Re_3F_3 with different symmetries and different spin states are the minima on the B3LYP potential energy surfaces with all real vibrational frequencies. The theoretical studies show that the global minimum for Re_3F_3 has a completely arbitrary planar hexagonal structure. The ground state of Re_3F_3 is found to be quintet state $^5A'$ with the C_s symmetry. We further located one

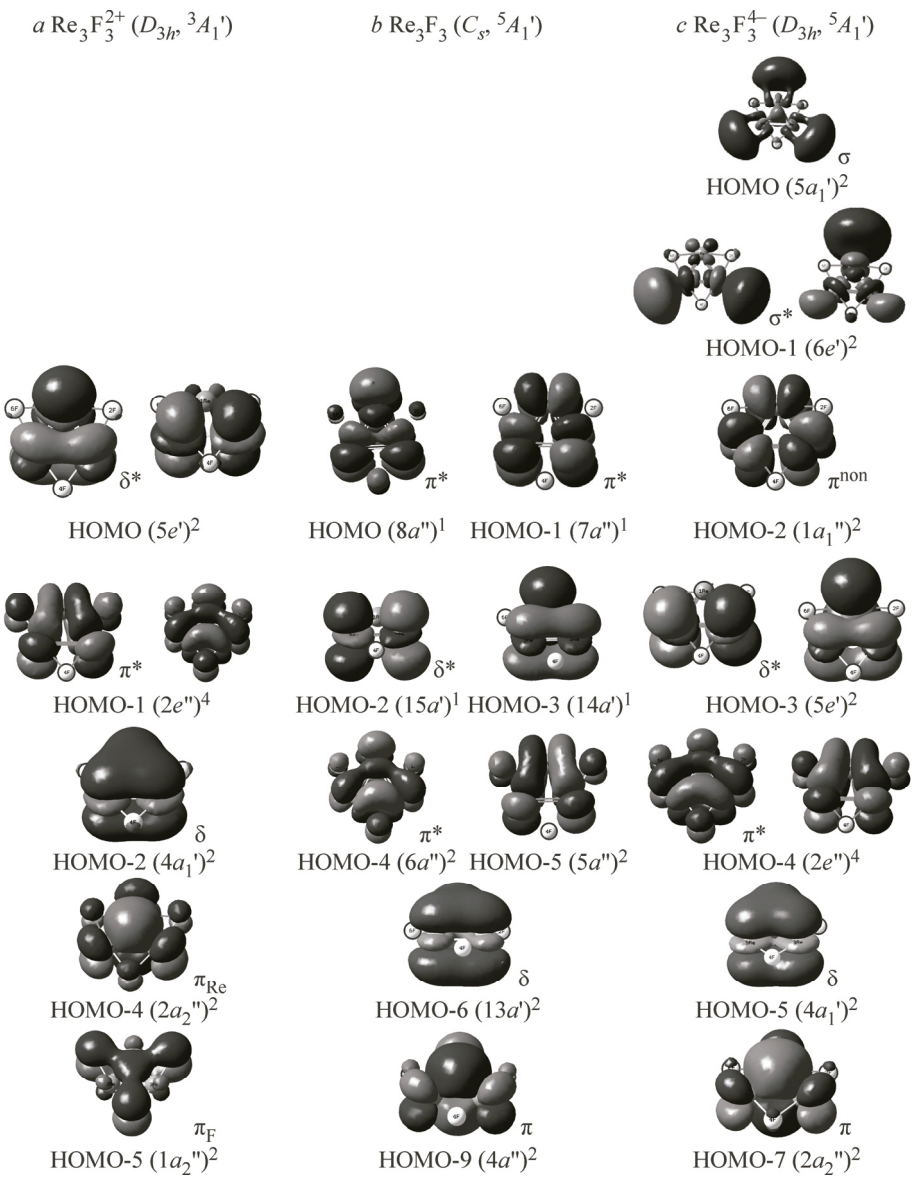

Fig. 2. Six top MOs in $Re_3F_3^{2+}$ (D_{3h}, $^3A_{1'}$), ten top MOs in Re_3F_3 (C_s, $^5A'$), and eight top MOs in $Re_3F_3^{4-}$ (D_{3h}, $^5A_{1'}$)

low-lying singlet state D_{3h} ($^1A_1'$) and one low-lying triplet state C_{2v} ($^3B_1$) for Re_3F_3 by 0.302 eV and 0.299 eV above the ground state, respectively. The heptet state (C_{2v}, $^7B_2$) is found to be 0.185 eV above the ground state. A detailed MO analysis at the rear reveals that the Re_3F_3 (C_s, $^5A'$) cluster possesses multiple aromaticity that is responsible for the high spin multiplicity of the $^5A'$ structure. As seen from Table 1, the Re—Re bond length is 2.317 ~ 2.414 Å for the ground state of the Re_3F_3 (C_s, $^5A'$) cluster. The Re—Re bond length is lower than the sum (2.56 Å) of Re and Re covalent radii. The bond length of the planar arbitrary hexagonal Re_3F_3 (C_s, $^5A'$) cluster provides the structural criteria of its aromaticity. The bond lengths support the formation of a delocalized effect on the completely arbitrary triangular Re_3 framework. It goes without saying that the Re—Re bond of the planar arbitrary triangular Re_3 framework is a completely delocalized three-center metal-metal single bonding. WBI also provides some information about the existence of a ring current. The calculated WBI values of Re—Re for the ground state of the Re_3F_3 (C_s, $^5A'$) cluster are 1.214 ~ 2.068, which is between the standard

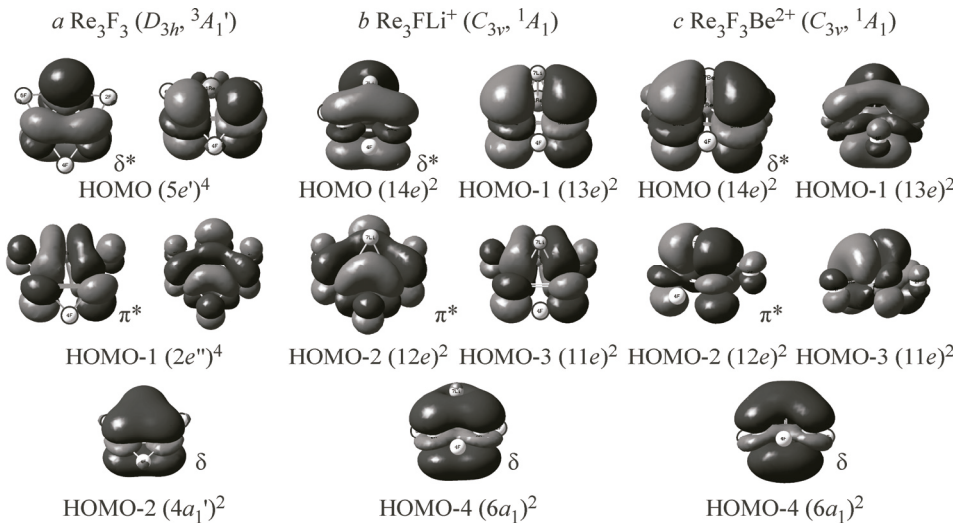

Fig. 3. Five top MOs in $Re_3F_3Li^+$ and $Re_3F_3Be^{2+}$ (C_{3v}, $^1A_1$) (Three top MOs in Re_3F_3 (D_{3h}, $^1A_{1'}$) are given for comparison)

values of a single bond (1.0) and a double bond (2.0). The WBI values support the formation of a delocalized effect on the planar arbitrary triangular Re_3 framework and the aromatic nature of the Re_3F_3 (C_s, $^5A'$) cluster.

We also performed an extensive search for the $Re_3F_3^{2+}$ dication global minimum with different spin multiplicities and different symmetries at the B3LYP level of theory. Our theoretical results clearly show that the global minimum of the $Re_3F_3^{2+}$ dication has a perfect D_{3h} ($^3A_1'$) planar regular hexagonal structure. Therefore, the ground state of $Re_3F_3^{2+}$ is found to be triplet state $^3A_1'$ with the D_{3h} symmetry. The Re—Re bond lengths are 2.330 Å and the Re—F bond lengths are 2.067 Å. The Re—Re bond length is lower than the sum (2.560 Å) of Re and Re covalent radii. The bond length value provides the structural criteria of aromaticity in the $Re_3F_3^{2+}$ (D_{3h}, $^3A_1'$) dication. The calculated WBI of Re—Re for the ground state of $Re_3F_3^{2+}$ is 1.940, which is between the standard values of a single bond (1.0) and a double bond (2.0). WBI of Re—Re for the $Re_3F_3^{2+}$ (D_{3h}, $^3A_1'$) dication supports the formation of a delocalized effect on the planar equilateral triangular Re_3 framework and therefore the aromatic nature of the planar regular hexagonal structure for the $Re_3F_3^{2+}$ (D_{3h}, $^3A_1'$) dication. The population analysis using the SCF density shows that the occupied alpha orbital symmetry configuration of the $Re_3F_3^{2+}$ (D_{3h}, $^3A_1'$) ground state is $1a_1'1e'2e'2a_1'1e''3a_1'1a_2'3e'1a_2''2a_2''4e'4a_1'2e''5e'$.

For the $Re_3F_3^{4-}$ cluster five geometric isomers were obtained, which had different spin states and symmetries (Table 1). The ground state of $Re_3F_3^{4-}$ is found to be quintet state $^5A_1'$ (D_{3h}) with the lowest energy and the highest symmetry. This structure is based on a regular planar hexagon and the Re—Re and Re—F bond lengths are 2.426 and 2.156 Å. Similarly, the Re—Re bond length is lower than the sum (2.56 Å) of Re and Re covalent radii. It supports the formation of a delocalized effect on the equilateral triangular Re_3 framework. An isosceles hexagonal C_{2v} ($^3B_2$) structure with a triplet state is found to be only 0.136 eV above the ground state. We further located two low-lying D_{3h} symmetries: D_{3h} ($^3A_1'$) and D_{3h} ($^1A_1'$) for the $Re_3F_3^{4-}$ cluster, 0.789 and 0.735 eV above the ground state, respectively, whereas the heptet state (C_s, $^7A'$) is 0.218 eV above the ground state. Our theoretical results clearly show that the $Re_3F_3^{4-}$ cluster has a propensity to adopt the quintet state D_{3h} ($^5A_1'$) ground state. The high spin ground state for the $Re_3F_3^{4-}$ cluster is quite remarkable. The population analysis using the

SCF density shows that the occupied alpha orbital symmetry configuration of the $Re_3F_3^{4-}$ (D_{3h}, $^5A_1'$) global minimum is $1a_1'1e'2a_1'2e'1e''3e'1a_2'1a_2''3a_1'2a_2''4e'4a_1'2e''5e'1a_1''6e'5a_1'$. A detailed MO analysis at the rear reveals that the occupied alpha orbitals of $Re_3F_3^{4-}$ (D_{3h}, $^5A_1'$) possess multiple (σ and partially δ) aromaticity. Comparing the perfect D_{3h} structure of $Re_3F_3^{4-}$ with that of the $Re_3F_3^{2+}$ dication, we obtain that the Re—F bond length of $Re_3F_3^{4-}$ is larger (0.09 Å) than that of the $Re_3F_3^{2+}$ dication. This is due to the additional six electrons occupying HOMO ($5a_1'$), HOMO-1 ($6e'$), and HOMO-2 ($1a_1''$) of $Re_3F_3^{4-}$ (D_{3h}, $^5A_1'$). The HOMO ($5a_1'$) is a fully occupied σ orbital with two σ electrons, which will lead to σ aromaticity in $Re_3F_3^{4-}$ (D_{3h}, $^5A_1'$).

MO analysis for the $Re_3F_3^{2+}$ (D_{3h}, $^3A_1'$), Re_3F_3 (C_s, $^5A'$), and $Re_3F_3^{4-}$ (D_{3h}, $^5A_1'$) clusters. To further understand the electronic structure and chemical bonding in $Re_3F_3^{2+}$ (D_{3h}, $^3A_1'$), Re_3F_3 (C_s, $^5A'$), and $Re_3F_3^{4-}$ (D_{3h}, $^5A_1'$) clusters, we carried out a detailed MO analysis for their ground states. Similar to the $Re_3O_3^{23-}$ ground state, the C_s global minimum structure for the Re_3F_3 (C_s, $^5A'$) ground state is very different from the highly symmetric D_{3h} structure of aromatic $Ta_3O_3^{34-}$ and $Hf_3F_3^{33-}$ clusters. The origin of the reduced symmetry in Re_3F_3 (C_s, $^5A'$) can be understood from an analysis of its valence electronic structure. The Re atom possesses electron configuration $5d^56s^2$. The top eleven occupied valence orbitals in the Re_3F_3 (C_s, $^5A'$) ground state are Re-based *s*—*d* orbitals, as shown in Fig. 3, *b*. Among the eleven MOs, three are responsible for the σ bonding of the triangular Re_3 framework. They include completely bonding HOMO-10 (10*a*′) and partially bonding/antibonding HOMO-8 (11*a*′) and HOMO-7 (12*a*′). The antibonding nature of HOMO-8 (11*a*′) and HOMO-7 (12*a*′) significantly reduces the σ bonding HOMO-10 (10*a*′) contribution to the Re_3 framework, and thus they would almost cancel each other. HOMO-9 (4*a*″) is a completely bonding π orbital, HOMO-5 (5*a*″) and HOMO-4 (6*a*″) are two partially bonding/antibonding π* orbitals, HOMO-1 (7*a*″) is a nonbonding π^{non} orbital, and HOMO (8*a*″) is also a partially bonding/antibonding π* orbital in the Re_3F_3 (C_s, $^5A'$) cluster. These five MOs of the Re_3F_3 (C_s, $^5A'$) cluster constitute a set of bonding, antibonding, and nonbonding orbitals composed of the same Re $5d_{yz}$ and $5d_{xz}$ hybrid functions. When all bonding, antibonding, and nonbonding MOs composed of the same AOs (such as the Re $5d_{yz}$ and $5d_{xz}$ orbitals in this case) are occupied, the net bonding effect is expected to be zero and this set MOs can be viewed as atomic lone pairs [35]. If therein the antibonding or nonbonding MOs are half-filled, the net bonding effect of this set of MOs will be approximately zero. The set of HOMO-9 (4*a*″), HOMO-7(5*a*″), HOMO-4 (6*a*″) and HOMO-1 (7*a*″), and HOMO (8*a*″) do not contribute to the net bonding in the Re_3F_3 (C_s, $^5A'$) cluster. The most interesting MO is HOMO-6 (13*a*′) that is a completely bonding δ orbital. The 13*a*′ MO comes mainly from the overlap of the $5d_{z^2}$ orbital on each Re atom. This orbital is symmetric with respect to the molecular plane and perpendicular to the molecular C_3 axis and has two nodal surfaces. HOMO-2 (15*a*′) and HOMO-3 (14*a*′) are two partial bonding/antibonding δ* orbitals. Thus, HOMO-4 (13*a*′), HOMO (15*a*′), and HOMO-3 (14*a*′) form a δ bonding/antibonding pair. HOMO-4 (13*a*′) is fully filled and HOMO-2 (15*a*′) and HOMO-3 (14*a*′) are half-filled, resulting in a partial δ bonding contribution to the Re_3F_3 (C_s, $^5A'$) cluster. The Re_3F_3 (C_s, $^5A'$) cluster can be considered to possess partial δ aromatic characters, which is the origin of the C_s ($^5A'$) global minimum structure. Our theoretical results clearly show that the Re_3F_3 (C_s, $^5A'$) cluster has a propensity to adopt a high spin state with low symmetry. The global minimum for Re_3F_3 (C_s, $^5A'$) is an open shell structure with a valence electronic configuration
$1a'^22a'^23a'^24a'^25a'^26a'^27a'^21a''^22a''^28a'^29a'^23a''^210a'^24a''^211a'^212a'^213a'^25a''^26a''^214a'^115a'^17a''^18a''^1$.

Our computational results also show that the global minimum D_{3h} ($^1A_1'$) for $Re_3F_3^{2+}$ has been proved to possess three types (σ, π, and δ) of the *d*-bonding interaction (as shown in Fig. 3, *a*) with electron configuration $1a_1'^21e'^42a_1'^22e'^41a_2'^23e'^41e''^41a_2''^23a_1'^22a_2''^24e'^44a_1'^22e''^45e'^4$. Because of the simi-

larity with Re_3F_3 in the structure, we explore the possibility of aromaticity in $Re_3F_3^{2+}$. The ground state of the $Re_3F_3^{2+}$ (D_{3h}, $^3A_1'$) dication is predicted to be an open shell with electron configuration $1a_1'^2 1e'^4 2e'^4 2a_1'^2 1e''^4 3a_1'^2 1a_2'^2 3e'^4 1a_2''^2 2a_2''^2 4e'^4 4a_1'^2 2e''^4 5e'^2$, which is formed by removing two electrons from the HOMO of Re_3F_3 (D_{3h}, $^1A_1'$). As shown in Figs. 4, *a* and 3, *a*, the top eight MOs of Re_3F_3 (D_{3h}, $^1A_1'$) were essentially maintained in the $Re_3F_3^{2+}$ (D_{3h}, $^3A_1'$) dication because only slight distortions are observed. The fully occupied HOMO-8 ($3a_1'$) of the $(Re_3F_3)^{2+}$ (D_{3h}, $^3A_1'$) dication is a σ bonding MO, and the fully occupied HOMO-3 ($4e'$) of the $Re_3F_3^{2+}$ (D_{3h}, $^3A_1'$) dication are two partially bonding/antibonding doubly degenerate σ* orbitals. They form a σ bonding/antibonding pair, due to that HOMO-3 ($4e'$) and HOMO-8 ($3a_1'$) are composed of the same *s*-*d* hybrid functions. They would almost cancel each other, thus resulting in negligible metal-metal σ bonding in the $Re_3F_3^{2+}$ (D_{3h}, $^3A_1'$) dication. Analogously, the fully occupied HOMO-4 ($2a_2''$) and HOMO-1 ($2e''$) of $Re_3F_3^{2+}$ (D_{3h}, $^3A_1'$) are π and π* orbitals, respectively, which form a π bonding/antibonding pair and do not contribute to the net chemical bonding in the $Re_3F_3^{2+}$ (D_{3h}, $^3A_1'$) dication. The HOMO-2 ($4a_1'$) and HOMO ($5e'$) of $Re_3F_3^{2+}$ (D_{3h}, $^3A_1'$) are δ bonding and δ* antibonding orbitals, respectively, which are formed by removing two electrons from the $5e'^4$ HOMO of Re_3F_3 (D_{3h}, $^1A_1'$). These three orbitals form a δ bonding/antibonding pair. The antibonding $5e'$ HOMO is half-filled, resulting in a partial δ bonding contribution, which is responsible for the triangular Re_3 framework. The remaining one valence MO of the $Re_3F_3^{2+}$ (D_{3h}, $^3A_1'$) dication is HOMO-5 ($1a_2''^2$), and the overlap of the $2p_z$-orbitals of three fluoride atoms generates a bonding $1a_2''$ π-MO with two π electrons. The two delocalized π electrons indicate that the $Re_3F_3^{2+}$ (D_{3h}, $^3A_1'$) dication can be considered as π_F aromatic according to the $(4n+2)$ Hückel rule, which is responsible for the triangular F_3 framework. In the present studies, the $Re_3F_3^{2+}$ (D_{3h}, $^3A_1'$) dication is the first example of π aromaticity composed of the p_z AOs of three nonmetal atoms in transition metal and nonmetal compounds. The $Re_3F_3^{2+}$ (D_{3h}, $^3A_1'$) dication is an unusual case of combining $5d_{z^2}$ orbital partial δ aromaticity of Re_3 with $2p_z$ orbital π aromaticity of F_3. Thus, the $Re_3F_3^{2+}$ (D_{3h}, $^3A_1'$) dication can be considered to possess the multiple (π_F and partial δ) aromatic character.

As depicted in Fig. 3, *c*, the $3a_1'$, $4e'$, and $6e'$ MOs of the $Re_3F_3^{4-}$ (D_{3h}, $^5A_1'$) ground state form a σ bonding/antibonding pair and should not significantly contribute to the net aromaticity. The $2a_2''$, $2e''$, and $1a_1''$ MOs form a set of π bonding/antibonding/nonbonding MOs composed of the same Re $5d_{z^2}$, $5d_{yz}$, and $5d_{xz}$ hybrid functions, and should not contribute to the net aromaticity. The $4a_1'$ and $5e'$ MOs are completely δ bonding and partially δ* bonding/antibonding MOs. The bonding $4a_1'$ MO is fully filled and the bonding/antibonding $5e'$ MOs are half-filled, resulting in a partial δ aromaticity contribution to $Re_3F_3^{4-}$ (D_{3h}, $^5A_1'$). The most interesting MO is HOMO ($5a_1'$), which is a completely bonding σ_r orbital composed of $5d_{xy,\,x^2-y^2}$ AOs from each Re atom. The two delocalized electrons of the Re atom indicate that the $Re_3F_3^{4-}$ (D_{3h}, $^5A_1'$) cluster can be considered as σ_r aromaticity according to the $(4n+2)$ Hückel rule for σ aromaticity. Fig. 3, *c* shows that the fully occupied HOMO ($5a_1'$) indeed describes pure three-center two-electron (3*c*—2*e*) Re—Re σ_r bonding interactions with a very small contribution to the $Re_3F_3^{4-}$ (D_{3h}, $^5A_1'$) cluster. In conclusion, the $Re_3F_3^{4-}$ (D_{3h}, $^5A_1'$) cluster can be considered to possess multiple (σ and partial δ) aromatic characters.

$Re_3F_3X^+$ (C_{3v}, $^1A_1$) (X = Li, Na, K) and $Re_3F_3Y^{2+}$ (C_{3v}, $^1A_1$) (Y = Be, Mg, Ca) complexes. Geometric structures. Our studies on the $Re_3F_3X^+$ (C_{3v}, $^1A_1$) (X = Li, Na, K) and $Re_3F_3Y^{2+}$ (C_{3v}, $^1A_1$)

(Y = Be, Mg, Ca) complexes indicate that all Re—Re bond lengths are equal in the same species. As seen from Fig. 1, the Re—Re bond lengths are 2.341, 2.342, 2.339, and 2.358 Å, 2.360, 2.348 Å for $Re_3F_3Li^+$, $Re_3F_3Na^+$, $Re_3F_3K^+$, and $Re_3F_3Be^{2+}$, $Re_3F_3Mg^{2+}$, $Re_3F_3Ca_2^+$, respectively. These Re—Re bond lengths are lower than the sum (2.560 Å) of covalent radius for the Re and Re atoms. The Re—Re bond length of the regular triangular Re_3 framework in the Re_3F_3 (D_{3h}, $^1A_1'$) ligand of the hexagonal pyramidal $Re_3F_3X^+$ (C_{3v}, $^1A_1$) (X = Li, Na, K) and $Re_3F_3Y^{2+}$ (C_{3v}, $^1A_1$) (Y = Be, Mg, Ca) complexes provides the structural criteria of aromaticity. Except for the trend of all Re—Re bond lengths in the same structure to be equal, another trend can also be inferred from Fig. 2. The Re—Re bond lengths increase in the following order: Re_3F_3 (D_{3h}, $^3A_1'$) < $Re_3F_3Li^+$ < $Re_3F_3Na^+$ < $Re_3F_3K^+$ < $Re_3F_3Be^{2+}$ < < $Re_3F_3Mg^{2+}$ < $Re_3F_3Ca_2^+$. Based on the equation of all Re—Re bond lengths in the same conformation, we could conclude that in all species the Re_3 building block has a delocalized Re—Re bond and the strength of the metal-metal bond between Re and Re decreases in the above order. The above mentioned results can also be obtained from the analysis of $WBI_{Re—Re}$ in Table 1.

MO analysis. The electron structure and bonding nature in the hexagonal pyramidal $Re_3F_3X^+$ (C_{3v}, $^1A_1$) (X = Li, Na, K) and $Re_3F_3Y^{2+}$ (C_{3v}, $^1A_1$) (Y = Be, Mg, Ca) complexes can be also understood by analyzing their MOs. As depicted in Fig. 3, the MO numbers, shapes, and distribution and the bonding nature are completely the same in the hexagonal pyramidal $Re_3F_3Li^+$ (C_{3v}, $^1A_1$) and $Re_3F_3Be^{2+}$ (C_{3v}, $^1A_1$) complexes as the Re_3F_3 (D_{3h}, $^1A_1'$) ligand because only slight distortions are observed. The free Re_3F_3 (D_{3h}, $^1A_1'$) cluster and its $Re_3F_3X^+$ (C_{3v}, $^1A_1$) (X = Li, Na, K) and $Re_3F_3Y^{2+}$ (C_{3v}, $^1A_1$) (Y = Be, Mg, Ca) complexes are valence isoelectronic species and found to have the same singlet spin state. As shown in Fig. 3, *a*, fully occupied $3a_1'$, $2a_2''$ and $4a_1'$ in the free Re_3F_3 (D_{3h}, $^1A_1'$) cluster are σ bonding, π bonding, and δ bonding orbitals, respectively. Fully occupied $4e'$, $2e''$, and $5e'$ in the free Re_3F_3 (D_{3h}, $^1A_1'$) cluster are doubly degenerate σ* antibonding, π* antibonding, and δ* antibonding orbitals, respectively. The free Re_3F_3 (D_{3h}, $^1A_1'$) cluster possesses delocalized σ bonding, π-bonding, and δ bonding orbitals. This cannot make the aromatic nature of the Re_3F_3 (D_{3h}, $^1A_1'$) cluster because $4e'$ σ* antibonding, $2e''$ π* antibonding, and $5e'$ δ* antibonding orbitals exist in electron configuration $1a_1'^2 1e'^4 2a_1'^2 2e'^4 1a_2'^2 3e'^4 1e''^4 1a_2''^2 3a_1'^2 2a_2''^2 4e'^4 4a_1'^2 2e''^4 5e'^4$ of the free Re_3F_3 (D_{3h}, $^1A_1'$) cluster. It must affirm that the free Re_3F_3 (D_{3h}, $^1A_1'$) cluster possesses three types (σ, π, and δ) of the *d*-bonding interaction. As seen from Fig. 3, *b* and *c*, HOMO-4 ($6a_1$) of $Re_3F_3Li^+$ (C_{3v}, $^1A_1$) (or $Re_3F_3Be^{2+}$) is a completely delocalized δ bonding MO that mainly originates from the HOMO-2 ($4a_1'$) of free Re_3F_3 (D_{3h}, $^1A_1'$). The HOMO-7 ($5a_1$) of $Re_3F_3Li^+$ (C_{3v}, $^1A_1$) (or $Re_3F_3Be^{2+}$) is a completely delocalized π bonding MO that mainly originates from the HOMO-4 ($2a_2''$) of free Re_3F_3 (D_{3h}, $^1A_1'$). The fully occupied HOMO-8 ($4a_1$) of $Re_3F_3Li^+$ (C_{3v}, $^1A_1$) (or $Re_3F_3Be^{2+}$) is a completely delocalized σ bonding MO that mainly originates from the HOMO-5 ($3a_1'$) of free Re_3F_3 (D_{3h}, $^1A_1'$). Three MOs existing in $Re_3F_3Li^+$ (C_{3v}, $^1A_1$) or $Re_3F_3Be^{2+}$ (C_{3v}, $^1A_1$) are three types of the *d* bonding interaction, which is responsible for a three-center metal-metal bond of the triangular Re_3 framework in $Re_3F_3Li^+$ (C_{3v}, $^1A_1$) or $Re_3F_3Be^{2+}$ (C_{3v}, $^1A_1$). Similar results also exist in the $Re_3F_3Na^+$ (C_{3v}, $^1A_1$), $Re_3F_3K^+$ (C_{3v}, $^1A_1$), $Re_3F_3Mg^{2+}$ (C_{3v}, $^1A_1$), and $Re_3F_3Ca_2^+$ (C_{3v}, $^1A_1$) complexes. Our extensive DFT calculations reveal that the ground state of the Re_3F_3 (D_{3h}, $^1A_1'$) cluster possesses valence electronic configuration $1a_1'^2 1e''^4 2a_1''^2 2e''^4 1a_2'^2 3e''^4 1e''^4 1a_2''^2 3a_1'^2 2a_2''^2 4e''^4 4a_1'^2 2e''^4 5e'^4$ and the hexagonal pyramidal-type $Re_3F_3Li^+$ and $Re_3F_3Be^{2+}$ complexes are the (C_{3v}, $^1A_1$) structures with a valence electronic configuration $1a_1^2 1e^2 2e^2 2a_1^2 3e^2 4e^2 1a_2^2 5e^2 6e^2 3a_1^2 1a_2^2 7e^2 8e^2 4a_1^2 5a_1^2 9e^2 10e^2 6a_1^2 11e^2 12e^2 13e^2 14e^2$. Obviously, the Re_3F_3

(D_{3h}, $^1A_1'$) structural units were perfectly preserved in these $Re_3F_3X^+$ (C_{3v}, $^1A_1'$) (X = Li, Na, K and $Re_3F_3Y^{2+}$ (C_{3v}, $^1A_1'$) (Y = Be, Mg, Ca) complexes.

As depicted in Fig. 3, *b*, the Li center in $Re_3F_3Li^+$ (C_{3v}, $^1A_1$) is practically a naked atom. The calculated atomic natural electron configuration of Re $[Xe]6s^{0.59}5d^{5.62}6p^{0.03}6d^{0.02}$ and Li $[He]2s^{0.07}2p^{0.01}$ of $Re_3F_3Li^+$ (C_{3v}, $^1A_1$) support the metal-metal bonding of the Re—Re and Li—Re ionic interactions. Similar results also exist in the $Re_3F_3Na^+$ (C_{3v}, $^1A_1$), $Re_3F_3K^+$ (C_{3v}, $^1A_1$), $Re_3F_3Mg^{2+}$ (C_{3v}, $^1A_1$), and $Re_3F_3Ca_2^+$ (C_{3v}, $^1A_1$) complexes. Table 1 indicates that Re—Re and Re—F interactions are typical single bonds throughout the whole hexagonal pyramidal complexes, and $WBI_{Re—Re} \approx 1.804 – 1.430$ and $WBI_{Re—F} \approx 0.335 – 0.373$ were found. The X^+—Re_3F_3 (X = Li, Na, K) (or Y^{2+}—Re_3F_3 (Y = Be, Mg, Ca)) ionic interactions are clearly demonstrated by the fact that the alkali metal atom and the alkali-earth metal atom in these hexagonal pyramidal complexes possess high calculated natural atomic charges with $Q_{Li} = 0.904|e|$, $Q_{Na} = 0.938|e|$, $Q_K = 0.969|e|$, $Q_{Be} = 1.348|e|$, $Q_{Mg} = 1.589|e|$, and $Q_{Ca} = 1.754|e|$. The ionicity of these complexes increases from X = Li, Na to K and from Y = Be to Mg Ca, in line with the corresponding total WBIs that decrease from $WBI_{Li} = 0.188$, $WBI_{Na} = 0.122$ to $WBI_K = 0.064$ and from $WBI_{Be} = 1.090$, $WBI_{Mg} = 0.692$ to $WBI_{Ca} = 0.477$. The HOMO energy of the system is effectively lowered from –7.59 eV in free Re_3F_3 to –11.67 eV in $Re_3F_3Li^+$, –12.14 eV in $Re_3F_3Na^+$, –12.65 eV in $Re_3F_3K^+$, and –16.80 eV in $Re_3F_3Ca_2^+$, –17.88 eV in $Re_3F_3Mg^{2+}$, –18.96eV in $Re_3F_3Be^{2+}$ and the corresponding HOMO-LUMO energy gaps are greater than 7.51 eV in free Re_3F_3, which clearly provides evidence for the presence of a local ring-current effect on the Re_3 triangles and therefore the aromatic nature of the Re_3F_3 (D_{3h}, $^1A_1'$) ligand in these novel complexes.

CONCLUSIONS

We reported the theoretical studies on the rhenium low-fluoride $Re_3F_3^{2+/0/4-}$ clusters and its hexagonal pyramidal-type $Re_3F_3X^+$ (C_{3v}, $^1A_1'$) (X = Li, Na, K) and $Re_3F_3Y^{2+}$ (C_{3v}, $^1A_1'$) (Y = Be, Mg, Ca) complexes using DFT calculations. Comprehensive calculations are performed in search for the lowest energy structures of the $Re_3F_3^{2+}$ dication, neutral Re_3F_3, and $Re_3F_3^{4-}$ clusters. The ground state of $Re_3F_3^{2+}$ is found to be triplet state $^3A_1'$ $(1a_1'^2 1e'^4 2e'^4 2a_1'^2 1e''^4 3a_1'^2 1a_2'^2 3e'^4 1a_2''^2 2a_2''^2 4e'^4 4a_1'^2 2e''^4 5e'^2)$ with the D_{3h} symmetry; the ground state of Re_3F_3 is found to be quintet state $^5A'$ $(1a'^2 2a'^2 3a'^2 4a'^2 5a'^2 6a'^2 7a'^2 1a''^2 2a''^2 8a'^2 9a'^2 3a''^2 10a'^2 4a''^2 11a'^2 12'a_2 13a'^2 5a''^2 6a''^2 14a'^1 15a'^1 7a''^1 8a''^1)$ with the C_s symmetry, and the ground state of $Re_3F_3^{4-}$ is found to be quintet state $^5A_1'$ $(1a_1'^2 1e'^4 2a_1'^2 2e'^4 1e''^4 3e'^4 1a_2'^2 1a_2''^2 3a_1'^2 2a_2''^2 4e'^4 4a_1'^2 2e''^4 5e'^2 1a_1''^2 6e'^2 5a_1'^2)$ with the D_{3h} symmetry, respectively. A detailed MO analysis reveals that $Re_3F_3^{2+}$ (D_{3h}, $^3A_1'$) possesses multiple (π and partial δ) aromaticity responsible for a three-center bond of the triangular F_3 framework and the triangular Re_3 framework. The Re_3F_3 (C_s, $^5A'$) cluster possesses partial δ-aromaticity responsible for a three-center metal-metal bond of the triangular Re_3 framework. The $Re_3F_3^{4-}$ cluster possesses multiple (σ and partial δ) aromaticity responsible for a three-center metal-metal bond of the triangular Re_3 framework. The totally delocalized *d* orbital chemical bonding was discovered in the transition metal rich-oxidation state and transition-metal low-oxidation state clusters in the past. The results obtained in the present work provide other transition-metal low-fluoride $Re_3F_3^{2+/0/4-}$ clusters containing multiple (σ, π, and δ) aromaticity and its hexagonal pyramidal-type $Re_3F_3X^+$ (C_{3v}, $^1A_1$) (X = Li, Na, K) and $Re_3F_3Y^{2+}$ (C_{3v}, $^1A_1$) (Y = Be, Mg Ca) complexes also possess the corresponding three types of the *d* bonding interaction. It is worth noting that the $Re_3F_3^{2+}$ (D_{3h}, $^3A_1'$) dication is the first example of π orbital aromaticity composed of the $2p_z$ AOs of three nonmetal F atoms in the transition metal compound. These novel complexes may be targeted in future experiments to open a new area of coordination chemistry.

REFERENCES

1. *Cotton F.A., Curtis N.F., Harris C.B., Johnson B.F.G., Lippard S.J., Mague J.T., Robinson W.R., Wood J.S.* // Science. – 1964. – **145**. – P. 1305 – 1307.
2. *Cotton F.A., Mague J.T.* // Inorg. Chem. – 1964. – **3**. – P. 1402 – 1407.
3. *Cotton F.A., Lippard S.J.* // Inorg. Chem. – 1965. – **4**. – P. 59 – 65.
4. *Bennett M.J., Cotton F.A., Foxman B.M.* // Inorg. Chem. – 1968. – **7**. – P. 1563 – 1569.
5. *Rinke K., Schäfer H.* // Angew. Chem. – 1965. – **77**. – P. 131.
6. *Schäfer H., Rinke K., Rabeneck H.* // Z. Anorg. Allg. Chem. – 1974. – **403**. – P. 23 – 34.
7. *Rinke K., Klein M., Schäfer H.* // J. Less-Common Met. – 1967. – **12**. – P. 497 – 503.
8. *Sergeeva A.P., Boldyrev A.I.* // Comm. Inorg. Chem. – 2010. – **31**. – P. 2 – 12.
9. *Week P.F., Sergeeva A.P., Kim E., Boldyrev A.I., Czerwinski K.R.* // Inorg. Chem. – in press.
10. *Alvarbo-Soto L., Ramirez-Tagle R., Arratia-Perez R.* // Chem. Phys. Lett. – 2008. – **467**. – P. 94 – 96.
11. *Alvarbo-Soto L., Ramirez-Tagle R., Arratia-Perez R.* // J. Phys. Chem. A. – 2009. – **113**. – P. 1671 – 1673.
12. *Tsipis A.C., Depastas I.G., Karagiannis E.E., Tsipis C.A.* // J. Comput. Chem. – 2010. – **31**. – P. 431 – 446.
13. *Moulijn J.A., Mol J.C.* // J. Mol. Catal. – 1988. – **46**. – P. 1 – 14.
14. *Mol J.C.* // Catal. Today. – 1999. – **51**. – P. 289 – 299.
15. *Herrmann W.A., Kuchler J.G., Felixberger J.K., Herdtweck E., Wagner W.* // Angew. Chem. Int. Ed. – 1988. – **27**. – P. 394 – 396.
16. *Averkiev B.B., Boldyrev A.I.* // J. Phys. Chem. A. – 2007. – **111**. – P. 12864 – 12866.
17. *Wang B., Zhai H.J., Huang X., Wang L.S.* // J. Phys. Chem. A. – 2008. – **112**. – P. 10962 – 10967.
18. *Tanaka H., Neukemans S., Jansses E., Silverans R.E., Lievens P.* // J. Am. Chem. Soc. – 2003. – **125**. – P. 2862 – 2863.
19. *Höltzl T., Janssens E., Veldeman N., Veszprémi T., Lievens P., Nguyen M.T.* // Chem. Phys. Chem. – 2008. – **9**. – P. 833 – 838.
20. *Höltzl T., Veldeman N., Veszprémi T., Lievens P., Nguyen M.T.* // Chem. Phys. Lett. – 2009. – **469**. – P. 304 – 307.
21. *Wannere C.S., Corminboeuf C., Wang Z.X., Wodrich M.D., King R.B., Schlyer P.v.R.* // J. Am. Chem. Soc. – 2005. – **127**. – P. 5701 – 5705.
22. *Chen W.J., Zhai H.J., Huang X., Wang L.S.* // Chem. Phys. Lett. – 2011. – **512**. – P. 49 – 53.
23. *Zhai H.J., Chen W.J., Huang X., Wang L.S.* // RSC. Adv. – 2012. – **2**. – P. 2707 – 2712.
24. *Feng X.J., Cao T.T., Zhao L.X., Lei Y.M., Luo Y.* // Eur. Phys. J. D. – 2008. – **50**. – P. 285 – 288.
25. *Zubarev Y., Averkiev B.B., Zhai H.J., Wang L.S., Boldyrev A.I.* // Phys. Chem. Chem. Phys. – 2008. – **10**. – P. 257 – 267.
26. *Frisch M.J., Trucks G.W., Schlegel H.B., Scuseria G.E., Robb M.A., Cheeseman J.R., Montgomery J.A. Jr., Vreven T., Kudin K.N., Burant J.C., Millam J.M., Iyengar S.S., Tomasi J., Barone V., Mennucci B., Cossi M., Scalmani G., Rega N., Petersson G.A., Nakatsuji H., Hada M., Ehara M., Toyota K., Fukuda R., Hasegawa J., Ishida M., Nakajima T., Honda Y., Kitao O., Nakai H., Klene M., Li X., Knox J.E., Hratchian H.P., Cross J.B., Bakken V., Adamo C., Jaramillo J., Gomperts R., Stratmann R.E., Yazyev O., Austin A.J., Cammi R., Pomelli C., Ochterski J.W., Ayala P.Y., Morokuma K., Voth G.A., Salvador P., Dannenberg J.J., Zakrzewski G., Dapprich S., Daniels A.D., Strain M.C., Farkas O., Malick D.K., Rabuck A.D., Raghavachari K., Foresman J.B., Ortiz J.V., Cui Q., Baboul A.G., Clifford S., Cioslowski J., Stefanov B.B., Liu G., Liashenko A., Piskorz P., Komaromi I., Martin R.L., Fox D.J., Keith T., Al-Laham M.A., Peng C.Y., Nanayakkara A., Challacombe M., Gill P.M.W., Johnson B., Chen W., Wong M.W., Gonzalez C., Pople J.A.* Gaussian 03. – P. Revision C.01 ed., Gaussian, Inc., Pittsburgh, PA, 2003.
27. *Becke A.D.* // J. Chem. Phys. – 1993. – **98**. – P. 5648 – 5652.
28. *Lee C., Yang W., Parr R.G.* // Phys. Rev. B. – 1988. – **37**. – P. 785 – 789.
29. *Perdew J.P., Wang Y.* // Phys. Rev. B. – 1992. – **45**. – P. 13244 – 13249.
30. *Reed A.E., Curtiss L.A., Weinhold F.* // Chem. Rev. – 1988. – **88**. – P. 899 – 926.
31. *Reed A.E., Weinstock R.B., Weinhold F.* // J. Chem. Phys. – 1985. – **83**. – P. 735 – 747.
32. *Zhai H.J., Averkiev B.B., Zubarev D.Y., Wang L.S., Boldyrev A.I.* // Angew. Chem. – 2007. – **119**. – P. 4355 – 4358.
33. *Jin B., Jin Q.* // Comput. & Theoretical Chem. – 2013. – **1013**. – P. 130 – 135.
34. *Zhai H.J., Averkiev B.B., Zubarev D.Y., Wang L.S., Boldyrev A.I.* // Angew. Chem. Int. Ed. – 2007. – **46**. – P. 4277 – 4280.
35. *Boldyrev A.I., Wang L.S.* // Chem. Rev. – 2005. – **105**. – P. 3716 – 3757.